Peroxisome proliferator-activated receptor activity is involved in the osteoblastic differentiation regulated by bone morphogenetic proteins and tumor necrosis factor-α.

Mariko Takano, †Fumio Otsuka, Yoshinori Matsumoto, Kenichi Inagaki, Masaya Takeda, Eri Nakamura, Naoko Tsukamoto, Tomoko Miyoshi, Ken-ei Sada and Hirofumi Makino

Department of Medicine and Clinical Science, Okayama University Graduate School of Medicine, Dentistry and Pharmaceutical Sciences, 2-5-1 Shikata-cho, Kitaku, Okayama 700-8558, Japan

Running title: BMP and PPAR actions in osteoblast differentiation

Key words: bone morphogenetic protein (BMP), peroxisome proliferator-activated receptor (PPAR), osteoblast, and tumor necrosis factor-α (TNF-α)

Disclosure statement: All authors have nothing to disclose.

Correspondence to: †Fumio OTSUKA, M.D., Ph.D.
Endocrine Center of Okayama University Hospital,
2-5-1 Shikata-cho, Kitaku, Okayama 700-8558, Japan.
Phone: +81-86-235-7235, Fax: +81-86-222-5214
E-mail: fumiotsu@md.okayama-u.ac.jp

Abbreviations:

ALK, activin receptor-like kinase
ActRII, activin type-II receptor
BMP, bone morphogenetic protein; BMPRII, BMP type-II receptor
ERK, extracellular signal-regulated kinase
MAPK, mitogen-activated protein kinase
NFκB, nuclear factor-κB
IκB, inhibitory-κB
PPAR, peroxisome proliferator-activated receptor
SAPK/JNK, stress-activated protein kinase / c-Jun NH2-terminal kinase
TGF-β, transforming growth factor-β
TNF-α, tumor necrosis factor-α
TNFR, tumor necrosis factor receptor

ABSTRACT

Recent studies have suggested possible adverse effects of thiazolidinediones on bone metabolism. However, the detailed mechanism by which the activity of PPAR affects bone formation has not been elucidated. Impaired osteoblastic function due to cytokines is critical for the progression of inflammatory bone diseases. In the present study we investigated the cellular mechanism by which PPAR actions interact with osteoblast differentiation regulated by BMP and TNF-α using mouse myoblastic C2C12 cells. BMP-2 and -4 potently induced the expression of various bone differentiation markers including Runx2, osteocalcin, type-1 collagen and alkaline phosphatase (ALP) in C2C12 cells. When administered in combination with a PPARα agonist (fenofibric acid) but not with a PPARγ agonist (pioglitazone), BMP-4 enhanced osteoblast differentiation through the activity of PPARα. The osteoblastic changes induced by BMP-4 were readily suppressed by treatment with TNF-α. Interestingly, the activities of PPARα and PPARγ agonists reversed the suppression by TNF-α of osteoblast differentiation induced by BMP-4. Furthermore, TNF-α-induced

phosphorylation of MAPKs, NFκB, IκB and Stat pathways was inhibited in the presence of PPARα and PPARγ agonists with reducing TNF-α receptor expression. In view of the finding that inhibition of SAPK/JNK, Stat and NFκB pathways reversed the TNF-α suppression of osteoblast differentiation, we conclude that these cascades are functionally involved in the actions of PPARs that antagonize TNF-α-induced suppression of osteoblast differentiation. It was further discovered that the PPARα agonist enhanced BMP-4-induced Smad1/5/8 signaling through downregulation of inhibitory Smad6/7 expression, whereas the PPARγ agonist impaired this activity by suppressing BMPRII expression. On the other hand, BMPs increased the expression levels of PPARα and PPARγ in the process of osteoblast differentiation. Thus, PPARα actions promote BMP-induced osteoblast differentiation, while both activities of PPARα and PPARγ suppress TNF-α actions. Collectively, our present data establishes that PPAR activities are functionally involved in modulating the interaction between the BMP system and TNF-α receptor signaling that is crucial for bone metabolism.

INTRODUCTION

Bone morphogenetic proteins (BMPs), members of the transforming growth factor (TGF)-β superfamily, play pivotal regulatory roles in mesoderm induction and dorso-ventral patterning of developing limb buds and are known to promote differentiation of mesenchymal stem cells into chondrocytes and osteoblasts as well as differentiation of osteoprogenitor cells into osteoblasts (Lieberman et al., 2002). BMPs are also known to have critical roles in governing various aspects of embryological development, including development of the brain, heart, kidney and eyes (Reddi, 1997). In addition to the developmental actions of BMPs, various physiological actions of BMPs in endocrine and vascular tissues have recently been elucidated (Shimasaki et al., 2004; Otsuka, 2010; Otsuka et al., 2011). The biological functions of BMPs are mediated through the Smad signal transduction pathway via specific combinations of the proper BMP receptors (Shimasaki et al., 2004).

Osteoblast differentiation is a complex process regulated by various endocrine, paracrine and autocrine factors. Osteoblasts, which arise from mesenchymal stem cell

precursors, undergo differentiation in response to a number of factors, including BMPs, TGFs, insulin-like growth factor-I (IGF-I), vascular endothelial growth factor (VEGF), and steroids (McCarthy et al., 1989; Celeste et al., 1990; Midy and Plouet, 1994; Hughes et al., 1995; Spelsberg et al., 1999). Once matrix synthesis begins in cultured osteoblast cells, the cells differentiate and osteoblastic markers, including alkaline phosphatase (ALP), type-I collagen and osteocalcin, are subsequently activated. Osteoblasts then embed in the extracellular matrix consisting of collagen fibrils, and the matrix is mineralized and extended in collagen fibrils. Deposition and maintenance of mineralized skeletal elements are further regulated by various growth factors including BMPs and cytokines such as interleukins and tumor necrosis factors (TNFs).

Among the various cytokines, TNF-α receptor signaling plays a predominant role in bone loss in arthritis. TNF-α is also involved in controlling osteoblast survival and function in addition to the induction of osteoclast differentiation leading to bone resorption (Kudo et al., 2002). The effectiveness of blocking TNF-α actions in treatment of active rheumatoid arthritis established the clinical significance of TNF-α in the pathogenesis of inflammatory bone diseases (Feldmann and Maini, 2001; Scott and

Kingsley, 2006). However, the underlying mechanism of TNF-α in the regulation of differentiation of osteoblasts has not been fully elucidated.

Peroxisome proliferator-activated receptors (PPARs) including PPARα, PPARβ/δ and PPARγ are categorized to the family of nuclear hormone receptors (Desvergne and Wahli, 1999). PPARγ is activated by natural ligands such as polyunsaturated fatty acids and metabolites of prostaglandins and synthetic ligands, thiazolidinediones, such as rosiglitazone, pioglitazone and troglitazone (Willson et al., 2000). Recent studies have provided evidence that PPARγ activity may directly inhibit bone formation by diverting mesenchymal stem cells from the osteogenic process to the adipocytic lineage (Grey, 2008). Clinical studies have also revealed that thiazolidinediones decrease markers of bone formation with reduction in bone mass and increase in fracture incidence in women (Grey et al., 2007; Grey, 2008). However, the underlying mechanism by which PPARs affect osteoblastic differentiation has yet to be clarified.

The pluripotent mesenchymal precursor cell line, C2C12, a subclone of a mouse myoblastic cell line, has been widely used as a model to investigate the early

stages of osteoblast differentiation during bone formation in muscular tissues. Treatment of C2C12 cells with various TGF-β superfamily ligands has distinct effects on differentiation, and BMPs inhibit myoblast differentiation of C2C12 cells and promote osteoblastic cell differentiation (Katagiri et al., 1994; Ebisawa et al., 1999). In the present study, we investigated the cellular mechanisms by which PPAR agonists interact in the process of osteoblastic differentiation regulated by the activation of BMP and TNF-α with a focus on the interaction between BMP-Smad and PPAR signaling.

MATERIALS AND METHODS

Reagents and supplies

Dulbecco's Modified Eagle's Medium, penicillin-streptomycin solution, dimethylsulfoxide (DMSO), and the PPARα antagonist GW6471 were purchased from Sigma-Aldrich Co. Ltd. (St. Louis, MO). Recombinant human TNF-α was obtained from PeproTech EC Ltd. (London, UK). Recombinant human BMP-2, -4, -6 and -7 were purchased from R&D Systems, Inc. (Minneapolis, MN); ERK inhibitor U0126 and p38-MAPK inhibitor SB203580 were from Promega Corp. (Madison, WI); SAPK/JNK inhibitor SP600125 was from Biomol Lab. Inc. (Plymouth Meeting, PA); and the JAK family tyrosine kinase inhibitor AG490, Akt inhibitor SH-5 and NFκB activation inhibitor IV were from Calbiochem (San Diego, CA). Plasmids of BRE-Luc and Id-1-Luc were kindly provided by Drs. Tetsuro Watabe and Kohei Miyazono, Tokyo University, Japan. The PPARα agonist fenofibric acid and the PPARγ agonist pioglitazone were provided by Kaken Pharmaceutical Co. Ltd. (Tokyo, Japan) and Takeda Chemical Industries (Osaka, Japan), respectively.

Cell culture and morphological examination

The mouse myoblast cell line C2C12 was obtained from American Type Culture Collection (Manassas, VA). C2C12 cells were cultured in DMEM supplemented with 10% fetal calf serum (FCS) and penicillin-streptomycin solution at 37°C under a humid atmosphere of 95% air/5% CO_2. Changes in cell morphology were monitored using an inverted microscope.

RNA extraction, RT-PCR, and quantitative real-time PCR analysis

To prepare total cellular RNA, C2C12 cells were cultured in a 12-well plate (1×10^5 viable cells/well) and treated with the indicated concentrations of TNF-α and BMPs in combination with a PPARα agonist (fenofibric acid), a PPARγ agonist (pioglitazone) and various inhibitors including GW6471, U0126, SB203580, SP600125, AG490, NFκB inhibitor and SH-5 in serum-free DMEM. After 48-h culture, the medium was removed, and total cellular RNA was extracted using TRIzol® (Invitrogen Corp., Carlsbad, CA), quantified by measuring absorbance at 260 nm. The extracted RNA

(1.0 μg) was subjected to an RT reaction using the First-Strand cDNA synthesis system® (Invitrogen Corp.) with random hexamer (50 ng/μl), reverse transcriptase (200 U), and deoxynucleotide triphosphate (2.5 mM) at 42°C for 55 min and at 70°C for 10 min. Subsequently, hot-start PCR was performed using $MgCl_2$ (50 mM), deoxynucleotide triphosphate (2.5 mM), and 1.5 U of *Taq* DNA polymerase (Invitrogen Corp.) under the conditions we previously reported (Mukai et al., 2007; Matsumoto et al., 2010). PCR primer pairs, custom-ordered from Invitrogen Corp., were selected from different exons of the corresponding genes as follows: PPARα, 1769-1789 and 1950-1969 (from NM_011144); PPARγ, 567-588 and 838-858 (from NM_011146); Id-1, 225-247 and 364-384 (from NM_010495); runt-related transcription factor 2 (Runx2), 1041-1062 and 1379-1400 (from NM_009820); osteocalcin, 125-144 and 312-331 (NM_007541); type-1 collagen (collagen-1), 3872-3891 and 3922-3941 (NM_007742); ALP, 1365-1385 and 1549-1568 (NM_007431); TNFR1, 931-951 and 1211-1231 (BC052675); TNFR2, 142-162 and 1142-1162 (Y14622); and a house-keeping gene, ribosomal protein L19 (RPL19), 373-393 and 547-567 (from NM_009078). Primer pairs for mouse BMP type-1 and type-2 receptors and Smads were selected as we

reported previously (Otani et al., 2007; Takeda et al., 2007). The expression of PPARα, PPARγ and RPL19 mRNAs was detected by RT-PCR analysis. Aliquots of PCR products were electrophoresed on 1.5% agarose gels and visualized after ethidium bromide staining. For the quantification of mRNA levels of PPARs, Runx2, osteocalcin, collagen-1, ALP, TNFRs, BMP receptors, Smads and Id-1, real-time PCR was performed using the StepOnePlus® real-time PCR system (Applied Biosystems, Foster City, CA) under optimized annealing conditions, following the manufacturer's protocol with the following profile: 40 cycles each at 95°C for 3 sec and 60-62°C for 30 sec. The threshold cycle (Ct) values were calculated using the StepOnePlus™ system software (Applied Biosystems). The relative expression of each mRNA was calculated by the ΔCt method, in which ΔCt is the value obtained by subtracting the Ct value of RPL19 mRNA from the Ct value of the target mRNA, and the amount of target mRNA relative to RLP19 mRNA was expressed as $2^{-(\Delta Ct)}$. The data are expressed as the ratio of target mRNA to RPL19 mRNA.

Western immunoblot analysis

Cells (1×10^5 viable cells/well) were precultured in 12-well plates in DMEM containing 10% FCS for 24 h. After preculture, the medium was replaced with serum-free fresh medium, and then cells were treated with the indicated concentrations of the PPARα agonist (fenofibric acid) and PPARγ agonist (pioglitazone) for 24 h before addition of TNF-α and BMP-4. After stimulation with growth factors for 15 and 60 min, cells were solubilized in 100 μl RIPA lysis buffer (Upstate Biotechnology, Inc., Lake Placid, NY) containing 1 mM Na_3VO_4, 1 mM sodium fluoride, 2% sodium dodecyl sulfate, and 4% β-mercaptoethanol. For detecting protein expression of PPARα and PPARγ, cell lysates were collected from cells treated with BMP-4 for 48 h and 72 h. For detecting protein expression of TNFRs, cell lysates were collected from cells treated with PPARα and PPARγ agonists for 48 h. The cell lysates were then subjected to SDS-PAGE/immunoblotting analysis as we previously reported using anti-phospho-Smad1/5/8 antibody (Cell Signaling Technology, Inc., Beverly, MA), anti-phospho- and anti-total-extracellular signal-regulated kinase (ERK) 1/2 MAPK antibodies (Cell Signaling Technology, Inc.), anti-phospho- and anti-total-p38 MAPK antibodies (Cell Signaling Technology, Inc.), anti-phospho- and

anti-total-stress-activated protein kinase/c-Jun NH2-terminal kinase (SAPK/JNK) MAPK antibodies (Cell Signaling Technology, Inc.), anti-phospho- and anti-total NFκB-p65 antibodies, and anti-phospho- and anti-total IκB-α antibodies (Cell Signaling Technology, Inc.), anti-phospho- and anti-total-Stat3 and Stat5 antibodies (Cell Signaling Technology, Inc.), anti-phospho- and anti-total-Akt antibodies (Cell Signaling Technology, Inc.), anti-PPARα (H-98) and anti-PPARγ (H-100) antibodies (Santa Cruz Biotechnology, Inc., Santa Cruz, CA), anti-TNFR1 (H-271) and anti-TNFR2 (H-202) antibodies (Santa Cruz Biotechnology, Inc.), and anti-actin antibody (Sigma-Aldrich Co. Ltd.). The relative integrated density of each protein band was digitized by NIH image J 1.34s.

Transient transfection and luciferase assay

C2C12 cells (5×10^4 viable cells) were precultured in 12-well plates in DMEM with 10% FCS. The cells were then transiently transfected with 500 ng of BRE-Luc or Id-1-Luc reporter plasmids and 50 ng of cytomegalovirus-β-galactosidase plasmid (pCMV-β-gal) using FuGENE 6 (Roche Molecular Biochemicals, Indianapolis, IN) for

12 h. The cells were then treated with the indicated concentrations of PPARα and PPARγ agonists in combination with BMP-4 in serum-free fresh medium for 24 h. The cells were washed with PBS and lysed with Cell Culture Lysis Reagent (Toyobo, Osaka, Japan). Luciferase activity and β-galactosidase (β-gal) activity of the cell lysate were measured by luminescencer-PSN (ATTO, Tokyo, Japan). The data are shown as the ratio of luciferase to β-gal activity.

Statistical analysis

All results are shown as means ± SEM of data from at least three separate experiments, each performed with triplicate samples. Differences between groups were analyzed for statistical significance using ANOVA with Fisher's protected least significant difference (PLSD) test or unpaired *t*-test, when appropriate, to determine differences (StatView 5.0 software, Abacus Concepts, Inc., Berkeley, CA). *P* values < 0.05 were accepted as statistically significant.

RESULTS

We first examined the effects of PPAR agonists on BMP-induced osteoblastic differentiation of C2C12 cells. BMP ligands including BMP-2, -4, -6 and -7 (100 ng/ml) facilitated osteoblastic differentiation of C2C12 cells for 48 h as demonstrated by the increased expression levels of Runx2, osteocalcin and type-1 collagen (collagen-1) mRNAs (**Fig. 1A**). BMP-2 and -4 (100 ng/ml) stimulated the expression of these bone differentiation markers more effectively than did the same concentrations of BMP-6 and -7. Of note, the presence of a PPARα agonist (fenofibric acid, 3 μM), but not a PPARγ agonist (pioglitazone, 3 μM), significantly enhanced osteoblast differentiation induced by BMP-4 (100 ng/ml) (**Fig. 1A**).

To know whether the effects of PPARα agonist (fenofibric acid) on enhancing BMP-4-induced osteoblast differentiation occurred through PPARα, a specific antagonist of PPARα, GW6471, was used in the same culture conditions. As shown in **Fig. 1B**, the effects of PPARα agonist (3 μM) on Runx2 and collagen-1 expression induced by BMP-4 (100 ng/ml) were reversed in the presence of GW6471 (1 to 10 μM)

concentration dependently.

To elucidate the mechanism by which PPAR agonists modulate the expression levels of osteoblastic markers in C2C12 cells, effects of PPAR agonists on BMP receptor signaling were subsequently examined. It was found that the PPARα agonist (3 μM) significantly enhanced promoter activity of the BMP-responsive element represented by BRE-Luc activity induced by BMP-4 (100 ng/ml) (**Fig. 1C**). In contrast, the PPARγ agonist (3 μM) reduced BRE-Luc activity induced by BMP-4 (100 ng/ml) (**Fig. 1C**). Similar results were obtained by a promoter assay using the BMP target gene Id-1-Luc (data not shown). Furthermore, the PPARα agonist (3 μM) significantly reduced mRNA levels of inhibitory Smad6 and Smad7, while treatment with the PPARγ agonist (3 μM) decreased the expression level of BMPRII mRNA in C2C12 cells (**Fig. 1D**). With regard to the BMP receptor system, several preferential combinations of BMP ligands and receptors have been recognized to date (Shimasaki et al., 2004). BMP-2 and -4 most readily bind to ALK-3 and/or ALK-6 in combination with the type-2 receptor BMPRII. Since ALK-6 is not expressed in C2C12 cells (Mukai et al., 2007), the major functional complex for the osteoblastic differentiation

induced by BMP-4 is likely ALK-3/BMPRII. Thus, PPARγ activity was found to suppress BMP-Smad signaling by inhibiting BMPRII expression, whereas PPARα enhanced BMP receptor signaling by suppressing inhibitory Smad6/7. On the other hand, BMP-2, -4, -6 and -7 (100 ng/ml) induced increases in mRNA levels of PPARα and PPARγ in C2C12 cells cultured for 48 h (**Fig. 1E**). It was also found that BMP-4 (100 ng/ml) stimulated the expression of PPARα and PPARγ protein levels in 48 h to 72 h cultures (**Fig. 1F**).

We next studied the effects of PPAR activities on the interaction between BMP and TNF-α in C2C12 cells. Osteoblastic differentiation induced by BMP-2, -4, -6 and -7 (100 ng/ml) was suppressed by co-treatment with TNF-α (10 ng/ml), with the most pronounced effects on BMP-2- and BMP-4-induced differentiation (**Fig. 2A**). Importantly, the inhibitory effects of TNF-α (10 ng/ml) on BMP-4 (100 ng/ml)-induced mRNA expression of osteoblastic markers including Runx2, osteocalcin and collagen-1 were reversed by co-treatment with PPARα and PPARγ agonists (3 μM), although the impact of PPARγ agonist on TNF-α inhibition of BMP-4-induced ALP expression was not significant (**Fig. 2B**). Smad1/5/8 phosphorylation induced by BMP-4 (100 ng/ml)

was suppressed by treatment with TNF-α (100 ng/ml) (**Fig. 2C**). Of note, the inhibitory actions of TNF-α (10 ng/ml) on BMP-induced Smad1/5/8 phosphorylation were reversed in the presence of either the PPARα or PPARγ agonist (3 μM) (**Fig. 2C**). In accordance with the results for Smad phosphorylation, suppression by TNF-α (10 ng/ml) of BMP target gene Id-1 transcription induced by BMP-4 was also partially reversed by co-treatment with PPARα and PPARγ agonists (3 μM) (**Fig. 2D**). The effects of TNF-α are mediated through two distinct receptors: type 1, also called p60/p55 receptor (TNFR1), and type 2, also called p80/p75 receptor (TNFR2) (Grell et al., 1994). PPARα and PPARγ agonists (3 μM) decreased the expression levels of TNFR1 and TNFR2 mRNAs (**Fig. 2E**). In addition, the changes in TNFR expression by PPARα and PPARγ agonist (3 μM) were evaluated by immunoblot analysis using anti-TNFR1 and TNFR2 antibodies, showing that the protein level of TNFR2 was also decreased by treatments with PPARα and PPARγ agonists (**Fig. 2F**). The mechanism by which PPARα/γ activities reduced TNF-α actions may be contributed to the downregulation of TNFR signaling in C2C12 cells. Thus, both actions of PPARα and PPARγ agonists antagonize suppression by TNF-α of osteoblastic differentiation

induced by BMP-4 with restoration of TNF-α-induced suppression of Smad1/5/8 phosphorylation and Id-1 transcription.

Subsequently, the effects of PPARα and PPARγ agonists on TNF-α-induced cellular signaling were investigated. TNF-α (100 ng/ml) readily stimulated MAPK phosphorylation including ERK1/ERK2, p38-MAPK, SAPK/JNK pathways in C2C12 cells (**Fig. 3A**). The TNF-α actions were not significantly altered by treatment with BMP-4 (100 ng/ml). Notably, TNF-α (100 ng/ml)-induced phosphorylation of MAPKs including p38-MAPK and SAPK/JNK pathways (**Fig. 3A**) was inhibited in the presence of either the PPARα or PPARγ agonist (3 μM). NFκB, IκB and Stat3 pathways were also stimulated by TNF-α (100 ng/ml), and the stimulation of these pathways was not affected by co-treatment with BMP-4 (100 ng/ml) (**Fig. 3B)**. TNF-α-induced activation of NFκB signaling was significantly suppressed by the PPARγ agonist (3 μM), while IκB and Stat3 phoshorylation induced by TNF-α was inhibited by either the PPARα or PPARγ agonist (3 μM). The Akt pathway was also stimulated by TNF-α (100 ng/ml); however, PPARα or PPARγ agonist (3 μM) failed to suppress Akt phosphorylation (**Fig. 3B)**.

To further explore the major pathways for TNF-α receptor signaling in BMP-4-induced osteoblastic differentiation, cells were treated with specific inhibitors for ERK1/ERK2, p38-MAPK SAPK/JNK, Stat and NFκB. Inhibition of SAPK/JNK, Stat and NFκB pathways with SP600125, AG490 and NFκB inhibitor, respectively, reversed the suppression by TNF-α (10 ng/ml) of Runx2 (**Fig. 4A**) and osteocalcin (**Fig. 4B**) mRNA expression induced by BMP-4 (100 ng/ml). On the other hand, ERK1/ERK2 and p38 inhibition by U0126 and SB203580, respectively, failed to restore the suppression by TNF-α (10 ng/ml) of Runx2 (**Fig. 4A**) and osteocalcin (**Fig. 4B**) mRNA levels amplified by BMP-4 (100 ng/ml). We thus conclude that SAPK/JNK, Stat and NFκB signaling plays an important role in PPARα and PPARγ antagonizing the suppression by TNF-α of osteoblastic differentiation.

DISCUSSION

In the present study, we investigated the cellular mechanism by which PPAR agonists interact in osteoblastic differentiation regulated by BMP-4 and TNF-α using mouse myoblastic C2C12 cells. It was found that a PPARα agonist, fenofibric acid, stimulated BMP-4-induced osteoblastic differentiation through the PPARα activity. Of note, PPARα agonist was revealed to enhance BMP-4 receptor signaling by suppression of inhibitory Smad6/7 expression. TNF-α-induced SAPK/JNK, NFκB and Stat activation, which led to the inhibition of osteoblastic differentiation, was in turn inhibited by treatment with PPARα and PPARγ agonists. The present results demonstrate that PPARα actions promote osteoblastic differentiation induced by BMP-4, while both activities of PPARα and PPARγ are effective in suppressing TNF-α actions. In addition, BMPs also increased the sensitivity of PPAR agonists by upregulating the expression of PPARα and PPARγ in the process of osteoblastic differentiation. Hence, PPAR activities are functionally involved in modulating the interaction between BMP and TNF-α signaling, which is a key factor for osteoblastic differentiation (**Fig. 5**).

Although no bone abnormalities were identified in PPARα knockout mice (Wu et al., 2000), there is substantial evidence that PPARα has activities in bone development and in bone metabolism (Lecka-Czernik (Curr Osteoporos Rep 8: 84-90, 2010) provides a comprehensive review of relevant literature (Lecka-Czernik, 2010)). In particular, the collective data suggests that PPARα may regulate bone metabolism and bone marrow conditions by providing energy through fatty acid oxidation and by controlling cell commitment within hematopoietic lineages rather than affecting the differentiation of bone cells (Lecka-Czernik, 2010). Based on our present data, PPARα has beneficial effects, at least in part, in the early process of osteoblastic differentiation preferentially in combination with the activity of BMP-4, and both PPARα and PPARγ elicit anti-TNFα actions in the process of osteoblast differentiation.

PPARγ is a critical transcription factor for the induction of adipocyte differentiation based on the experimental and clinical studies using PPARγ agonists, thiazolidinediones (Grey, 2008). PPARγ transcripts are expressed in osteoblasts (Johnson et al., 1999; Jackson and Demer, 2000; Jeon et al., 2003) and osteoclast precursors (Mbalaviele et al., 2000; Chan et al., 2007). PPARγ agonists promote

adipogenesis instead of osteoblastogenesis *in vitro* (Gimble et al., 1996). PPARγ heterozygous-deficient mice demonstrate increased bone mass by stimulating osteoblastogenesis (Akune et al., 2004). Taken together, it appears that PPARγ activity preferentially promotes adipogenetic cascade instead of the process of osteoblastogenesis. In the present study, PPARγ activity was found to decrease Smad1/5/8 and its downstream signaling induced by BMP-4 by suppressing BMPRII expression in C2C12 cells, suggesting an inhibitory role of PPARγ activity in the early process of BMP-induced osteoblastic differentiation. However, the activity of PPARγ did not seem likely enough to attain the biological inhibition of BMP-induced osteoblast differentiation evaluated by the levels of Runx2, osteocalcin and collagen-1 expression. The interaction between PPAR and BMPs may be involved in the dual actions of adipogenesis and osteogenesis by BMPs. According to an analysis of BMPs on the mesenchymal stem cell differentiation, BMP-2, -4, -6, -7 and -9 activated adipogenic and osteogenic differentiation of mesenchymal stem cells (Kang et al., 2009). Interestingly, overexpression of PPARγ2 facilitated both osteogenic and adipogenic differentiation and PPARγ2 knockdown inhibited not only adipogenic differentiation but

also BMP-induced ossification (Kang et al., 2009), suggesting that PPARγ activity is also, at least in part, involved in promoting osteogenic differentiation.

Imbalanced functions of osteoclasts and osteoblasts lead to bone damage seen in patients with inflammatory bone diseases such as rheumatoid arthritis. Since bone loss in arthritis is related to activation of the TNF-α system, it can be hypothesized that TNF-α directly controls osteoblast survival and/or function in addition to its induction of osteoclast differentiation leading to excess bone resorption (Kudo et al., 2002). In this regard, we previously reported that TNF-α suppresses BMP-2-induced expression of osteoblast markers such as Runx2, osteocalcin and ALP (Mukai et al., 2007), in which MAPK and NFκB are involved in the suppression by TNF-α of BMP-2 activity in C2C12 cells (Mukai et al., 2007; Yamashita et al., 2008; Matsumoto et al., 2010). The present results further demonstrated that, among BMP ligands, BMP-4 most effectively augments PPARα activity leading to promotion of osteoblastic differentiation. BMP-4 also increased the sensitivity of PPAR agonists by upregulating the expression of PPARα and PPARγ in the process of osteoblastic differentiation. Moreover, the activities of PPARα and PPARγ are involved in

antagonizing the TNF-α signaling that is a negative factor for osteoblastic differentiation induced by BMP-4.

In our earlier study, the expression of other nuclear receptors such as estrogen receptors (ERα and ERβ) and glucocorticoid receptor (GCR) in C2C12 cells was significantly increased by BMP-2 stimulation (Matsumoto et al., 2010). BMP-2 increased the sensitivities of ERs and GCR, whereas estrogen and glucocorticoid differentially regulated BMP-Smad signaling, and these steroids antagonized TNF-α signaling in a different manner (Matsumoto et al., 2010). In the present study, in addition to ER and GCR actions, PPARs were also found to antagonize TNF-α activities in osteoblastic differentiation. Further studies are needed to utilize the efficacious actions of PPARα but modulate PPARγ activity in osteoblasts in relation to the activities of other nuclear receptor family molecules.

Collectively, PPARs are functionally involved in the process of osteoblast differentiation directed by BMP-4 and TNF-α. BMP-4 increases the sensitivities of PPARs, PPARα in turn upregulates and PPARγ represses BMP-Smad signaling, and PPARs antagonize TNF-α signaling in a different manner (**Fig. 5**). Understanding the

integrated mechanisms behind BMP- and TNF-α-regulated osteoblastic differentiation may lead to the development of novel therapeutic strategies for osteoporosis and/or inflammatory bone disorders.

ACKNOWLEDGEMENTS

We thank Dr. R. Kelly Moore for helpful discussion and critical reading of the manuscript. We are very grateful to Drs. Tetsuro Watabe and Kohei Miyazono, Tokyo University, Japan for providing BRE-Luc and Id-1-Luc plasmids. This work was supported in part by Grants-in-Aid for Scientific Research.

REFERENCES

Akune T, Ohba S, Kamekura S, Yamaguchi M, Chung UI, Kubota N, Terauchi Y, Harada Y, Azuma Y, Nakamura K, Kadowaki T, Kawaguchi H (2004) PPARgamma insufficiency enhances osteogenesis through osteoblast formation from bone marrow progenitors. J Clin Invest 113:846-855.

Celeste AJ, Iannazzi JA, Taylor RC, Hewick RM, Rosen V, Wang EA, Wozney JM (1990) Identification of transforming growth factor beta family members present in bone-inductive protein purified from bovine bone. Proc Natl Acad Sci U S A 87:9843-9847.

Chan BY, Gartland A, Wilson PJ, Buckley KA, Dillon JP, Fraser WD, Gallagher JA (2007) PPAR agonists modulate human osteoclast formation and activity in vitro. Bone 40:149-159.

Desvergne B, Wahli W (1999) Peroxisome proliferator-activated receptors: nuclear control of metabolism. Endocr Rev 20:649-688.

Ebisawa T, Tada K, Kitajima I, Tojo K, Sampath TK, Kawabata M, Miyazono K, Imamura T (1999) Characterization of bone morphogenetic protein-6 signaling pathways in osteoblast differentiation. J Cell Sci 112:3519-3527.

Feldmann M, Maini RN (2001) Anti-TNF alpha therapy of rheumatoid arthritis: what have we learned? Annu Rev Immunol 19:163-196.

Gimble JM, Robinson CE, Wu X, Kelly KA, Rodriguez BR, Kliewer SA, Lehmann JM, Morris DC (1996) Peroxisome proliferator-activated receptor-gamma activation by thiazolidinediones induces adipogenesis in bone marrow stromal cells. Mol Pharmacol 50:1087-1094.

Grell M, Zimmermann G, Hulser D, Pfizenmaier K, Scheurich P (1994) TNF receptors TR60 and TR80 can mediate apoptosis via induction of distinct signal pathways. J Immunol 153:1963-1972.

Grey A (2008) Skeletal consequences of thiazolidinedione therapy. Osteoporos Int 19:129-137.

Grey A, Bolland M, Gamble G, Wattie D, Horne A, Davidson J, Reid IR (2007) The peroxisome proliferator-activated receptor-gamma agonist rosiglitazone decreases bone formation and bone mineral density in healthy postmenopausal women: a randomized, controlled trial. J Clin Endocrinol Metab 92:1305-1310.

Hughes FJ, Collyer J, Stanfield M, Goodman SA (1995) The effects of bone morphogenetic protein-2, -4, and -6 on differentiation of rat osteoblast cells in vitro. Endocrinology 136:2671-2677.

Jackson SM, Demer LL (2000) Peroxisome proliferator-activated receptor activators modulate the osteoblastic maturation of MC3T3-E1 preosteoblasts. FEBS Lett 471:119-124.

Jeon MJ, Kim JA, Kwon SH, Kim SW, Park KS, Park SW, Kim SY, Shin CS (2003) Activation of peroxisome proliferator-activated receptor-gamma inhibits the Runx2-mediated transcription of osteocalcin in osteoblasts. J Biol Chem 278:23270-23277.

Johnson TE, Vogel R, Rutledge SJ, Rodan G, Schmidt A (1999) Thiazolidinedione effects on glucocorticoid receptor-mediated gene transcription and differentiation in osteoblastic cells. Endocrinology 140:3245-3254.

Kang Q, Song WX, Luo Q, Tang N, Luo J, Luo X, Chen J, Bi Y, He BC, Park JK, Jiang W, Tang Y, Huang J, Su Y, Zhu GH, He Y, Yin H, Hu Z, Wang Y, Chen L, Zuo GW, Pan X, Shen J, Vokes T, Reid RR, Haydon RC, Luu HH, He TC (2009) A comprehensive analysis of the dual roles of BMPs in regulating adipogenic and osteogenic differentiation of mesenchymal progenitor cells. Stem Cells Dev 18:545-559.

Katagiri T, Yamaguchi A, Komaki M, Abe E, Takahashi N, Ikeda T, Rosen V, Wozney JM, Fujisawa-Sehara A, Suda T (1994) Bone morphogenetic protein-2 converts the differentiation pathway of C2C12 myoblasts into the osteoblast lineage. J Cell Biol 127:1755-1766.

Kudo O, Fujikawa Y, Itonaga I, Sabokbar A, Torisu T, Athanasou NA (2002) Proinflammatory cytokine (TNFalpha/IL-1alpha) induction of human osteoclast formation. J Pathol 198:220-227.

Lecka-Czernik B (2010) PPARs in bone: the role in bone cell differentiation and regulation of energy metabolism. Curr Osteoporos Rep 8:84-90.

Lieberman JR, Daluiski A, Einhorn TA (2002) The role of growth factors in the repair of bone. Biology and clinical applications. J Bone Joint Surg Am 84-A:1032-1044.

Matsumoto Y, Otsuka F, Takano M, Mukai T, Yamanaka R, Takeda M, Miyoshi T, Inagaki K, Sada KE, Makino H (2010) Estrogen and glucocorticoid regulate osteoblast differentiation through the interaction of bone morphogenetic

protein-2 and tumor necrosis factor-alpha in C2C12 cells. Mol Cell Endocrinol 325:118-127.

Mbalaviele G, Abu-Amer Y, Meng A, Jaiswal R, Beck S, Pittenger MF, Thiede MA, Marshak DR (2000) Activation of peroxisome proliferator-activated receptor-gamma pathway inhibits osteoclast differentiation. J Biol Chem 275:14388-14393.

McCarthy TL, Centrella M, Canalis E (1989) Regulatory effects of insulin-like growth factors I and II on bone collagen synthesis in rat calvarial cultures. Endocrinology 124:301-309.

Midy V, Plouet J (1994) Vasculotropin/vascular endothelial growth factor induces differentiation in cultured osteoblasts. Biochem Biophys Res Commun 199:380-386.

Mukai T, Otsuka F, Otani H, Yamashita M, Takasugi K, Inagaki K, Yamamura M, Makino H (2007) TNF-alpha inhibits BMP-induced osteoblast differentiation through activating SAPK/JNK signaling. Biochem Biophys Res Commun 356:1004-1010.

Otani H, Otsuka F, Inagaki K, Takeda M, Miyoshi T, Suzuki J, Mukai T, Ogura T, Makino H (2007) Antagonistic effects of bone morphogenetic protein-4 and -7 on renal mesangial cell proliferation induced by aldosterone through MAPK activation. Am J Physiol Renal Physiol 292:F1513-1525.

Otsuka F (2010) Multiple endocrine regulation by bone morphogenetic protein system. Endocr J 57:3-14.

Otsuka F, McTavish K, Shimasaki S (2011) Integral role of GDF-9 and BMP-15 in ovarian function. Mol Reprod Dev 78:9-21.

Reddi AH (1997) Bone morphogenetic proteins: an unconventional approach to isolation of first mammalian morphogens. Cytokine Growth Factor Rev 8:11-20.

Scott DL, Kingsley GH (2006) Tumor necrosis factor inhibitors for rheumatoid arthritis. N Engl J Med 355:704-712.

Shimasaki S, Moore RK, Otsuka F, Erickson GF (2004) The bone morphogenetic protein system in mammalian reproduction. Endocr Rev 25:72-101.

Spelsberg TC, Subramaniam M, Riggs BL, Khosla S (1999) The actions and interactions of sex steroids and growth factors/cytokines on the skeleton. Mol Endocrinol 13:819-828.

Takeda M, Otsuka F, Otani H, Inagaki K, Miyoshi T, Suzuki J, Mimura Y, Ogura T, Makino H (2007) Effects of peroxisome proliferator-activated receptor activation on gonadotropin transcription and cell mitosis induced by bone morphogenetic proteins in mouse gonadotrope L β T2 cells. J Endocrinol 194:87-99.

Willson TM, Brown PJ, Sternbach DD, Henke BR (2000) The PPARs: from orphan receptors to drug discovery. J Med Chem 43:527-550.

Wu X, Peters JM, Gonzalez FJ, Prasad HS, Rohrer MD, Gimble JM (2000) Frequency of stromal lineage colony forming units in bone marrow of peroxisome proliferator-activated receptor-alpha-null mice. Bone 26:21-26.

Yamashita M, Otsuka F, Mukai T, Otani H, Inagaki K, Miyoshi T, Goto J, Yamamura M, Makino H (2008) Simvastatin antagonizes tumor necrosis factor-alpha inhibition of bone morphogenetic proteins-2-induced osteoblast differentiation by regulating Smad signaling and Ras/Rho-mitogen-activated protein kinase pathway. J Endocrinol 196:601-613.

FIGURE LEGENDS

Fig. 1. Effects of PPARα and PPARγ agonists on BMP-induced osteoblast differentiation. A) After preculture, C2C12 cells were treated with BMP-2, -4, -6 and -7 (100 ng/ml) in combination with PPARα and PPARγ agonists (3 μM) for 48 h. Total cellular RNA was extracted and then subjected to PCR reaction. Real-time PCR analysis was performed for quantification of Runx2, osteocalcin and collagen-1 mRNA levels. The expression levels of target genes were standardized by RPL19 level in each sample. B) Cells were treated with BMP-4 (100 ng/ml) in combination with PPARα agonist (3 μM) and the PPARα antagonist GW6471 (1 to 10 μM) for 48 h. Total cellular RNA was extracted and then subjected to real-time PCR analysis for quantification of Runx2 and collagen-1 mRNA levels. The expression levels of target genes were standardized by RPL19 level in each sample. C) Cells were transiently transfected with BRE-Luc reporter plasmid (500 ng) and pCMV-β-gal. The cells were then treated with BMP-4 (100 ng/ml) and with PPARα and PPARγ agonists (3 μM) for 24 h. The cells were lysed and the luciferase activity and β-galactosidase (β-gal)

activity were measured by a luminometer. The data were expressed as the ratio of luciferase to β-gal activity. D) Cells were treated with PPARα and PPARγ agonists (3 μM) for 48 h, and total cellular RNA was extracted. Real-time PCR analysis was performed for quantification of BMPRII, ActRII, ALK-2, ALK-3, Smad6 and Smad7 mRNA levels. The expression levels of target genes were standardized by RPL19 level in each sample. E) Cells were treated with BMP-2, -4, -6 and -7 (100 ng/ml) for 48 h, and total cellular RNA was extracted. Real-time PCR analysis was performed for quantification of PPARα and PPARγ mRNA levels. The expression levels of target genes were standardized by RPL19 level in each sample. F) For protein analysis, cells were treated with BMP-4 (100 ng/ml) for 48 h and 72 h. The cells were then lysed and subjected to SDS-PAGE/immunoblot (IB) analysis using antibodies that detect PPARα and PPARγ, and actin as an internal control. Results (A-E) are shown as means ± SEM of data from at least three separate experiments, each performed with triplicate samples. The results (F) shown are representative of those obtained from three independent experiments. The results were analyzed by ANOVA with Fisher's post hoc test (A-E). For each result within a panel, *, $P < 0.05$ vs. control in each set of

comparisons or between the indicated groups; and the values with different superscript letters are significantly different at $P < 0.05$.

Fig. 2. Effects of TNF-α and PPARα and PPARγ agonists on BMP-induced osteoblast differentiation and TNF receptor (TNFR) expression in C2C12 cells. A, B) After preculture, the cells were treated with BMP-2, -4, -6 and -7 (100 ng/ml), TNF-α (10 ng/ml), and PPARα and PPARγ agonists (3 μM) for 48 h. Total cellular RNA was extracted and subjected to PCR reaction. Real-time PCR analysis was performed for quantification of Runx2, osteocalcin, collagen-1 and ALP mRNA levels. The expression levels of target genes were standardized by RPL19 level in each sample. C) After preculture, the cells were pretreated with PPARα and PPARγ agonists (3 μM) for 24 h prior to addition of BMP-2 (100 ng/ml) and TNF-α (100 ng/ml). After 60-min culture, the cells were lysed and subjected to SDS-PAGE/immunoblot (IB) analysis using antibodies that detect phosphorylated Smad1/5/8 (pSmad1/5/8) and actin as an internal control. The results shown are representative of those obtained from three independent experiments. The relative integrated density of each protein band

was digitized by NIH image J 1.34s, pSmad1/5/8 levels were normalized by actin levels in each sample, and then pSmad1/5/8 levels after 60-min stimulation were expressed as fold changes. D) Cells were treated with BMP-4 (100 ng/ml) and TNF-α (10 ng/ml) in combination with PPARα and PPARγ agonists (3 μM) for 48 h and total RNA was extracted. Real-time PCR analysis was performed for the quantification of Id-1 mRNA levels. The expression levels of target genes were standardized by RPL19 level in each sample. E) Cells were treated with PPARα and PPARγ agonists (3 μM) for 48 h and total RNA was extracted. Real-time PCR analysis was performed for quantification of TNFR1 and TNFR2 mRNA levels. The expression levels of target genes were standardized by RPL19 level in each sample. F) For protein analysis, cells were treated with PPARα and PPARγ agonists (3 μM) for 48 h. The cells were then lysed and subjected to SDS-PAGE/immunoblot (IB) analysis using antibodies that detect TNFR1 and TNFR2, and actin as an internal control. The results shown are representative of those obtained from three independent experiments. Results (A-E) are shown as means ± SEM of data from at least three separate experiments, each performed with triplicate samples. The results were analyzed by the unpaired *t*-test

(A) or ANOVA with Fisher's post hoc test (B-E). For each result within a panel, *, $P < 0.05$ vs. control in each set of comparisons; and the values with different superscript letters are significantly different at $P < 0.05$.

Fig. 3. Effects of BMP-4 and PPARα and PPARγ agonists on TNF-α-induced MAPK, NFκB, IκB, Stat and Akt activation in C2C12 cells. A, B) After preculture, cells were treated with PPARα and PPARγ agonists (3 μM) for 24 h prior to addition of BMP-4 (100 ng/ml) and TNF-α (100 ng/ml). After 15- and 60-min culture, cells were lysed and subjected to SDS-PAGE/immunoblot (IB) analysis using anti-phospho- and anti-total-ERK1/ERK2 (pERK and tERK) antibodies, anti-phospho- and anti-total-p38 (pP38 and tP38) antibodies, anti-phospho- and anti-total-SAPK/JNK (pJNK and tJNK) antibodies, anti-phospho- and anti-total-NFκB-p65 (pNFκB and tNFκB) antibodies, anti-phospho- and anti-total-IκB (pIκB and tIκB) antibodies, anti-phospho- and anti-total-Stat3 (pStat3 and tStat3) antibodies, and anti-phospho- and anti-total-Akt (pAkt and tAkt) antibodies. The results (A, B) shown are representative of those obtained from three independent experiments. The relative integrated density of each

protein band was digitized by NIH image J 1.34s and shown as phospho-/total-protein levels in each panel. Results (A, B) are shown as means ± SEM of data from at least three separate experiments, each performed with triplicate samples. The results were analyzed by ANOVA with Fisher's post hoc test (A, B). For each result within a panel, the values with different superscript letters are significantly different at $P < 0.05$.

Fig. 4. Inhibitory effects of MAPK, NFκB, Stat and Akt pathways on Runx2 and osteocalcin expression regulated by BMP-2 and TNF-α. A, B) After preculture, cells were treated with BMP-4 (100 ng/ml) and TNF-α (10 ng/ml) in the presence or absence of indicated concentrations of the SAPK/JNK inhibitor SP600125, p38 inhibitor SB203580, ERK inhibitor U0126, JNK/STAT inhibitor AG490, NFκB activation inhibitor IV and Akt inhibitor SH-5 for 48 h and total cellular RNA was extracted. Real-time PCR was performed for quantification of Runx2 and osteocalcin mRNA levels. The expression levels of target genes were standardized by RPL19 level in each sample. Results (A, B) are shown as means ± SEM of data from at least three separate experiments, each performed with triplicate samples. The results were

analyzed by ANOVA with Fisher's post hoc test (A, B). For each result within a panel, the values with different superscript letters are significantly different at $P < 0.05$.

Fig. 5. Possible interaction of BMP-4, TNF-α and PPARs in the regulation of osteoblast differentiation. BMP-4 upregulates the expression of PPARα and PPARγ in C2C12 cells. A PPARα agonist, but not a PPARγ agonist, upregulates Runx2, osteocalcin and collagen-1 expression induced by BMP-4 through downregulating inhibitory Smads (Smad6/7) expression. On the other hand, the PPARγ agonist suppressed BMP type-2 receptor (BMPRII) expression, leading to impairment of BMP-Smad1/5/8 signaling. TNF-α-induced activation of MAPK, NFκB and Stat pathways suppresses the BMP-4-induced osteoblast differentiation. PPARα and PPARγ agonists reversed suppression by TNF-α of BMP-4-induced osteoblast differentiation through suppressing SAPK/JNK, NFκB and Stat signaling with reduction of TNF receptor expression.

Fig. 1

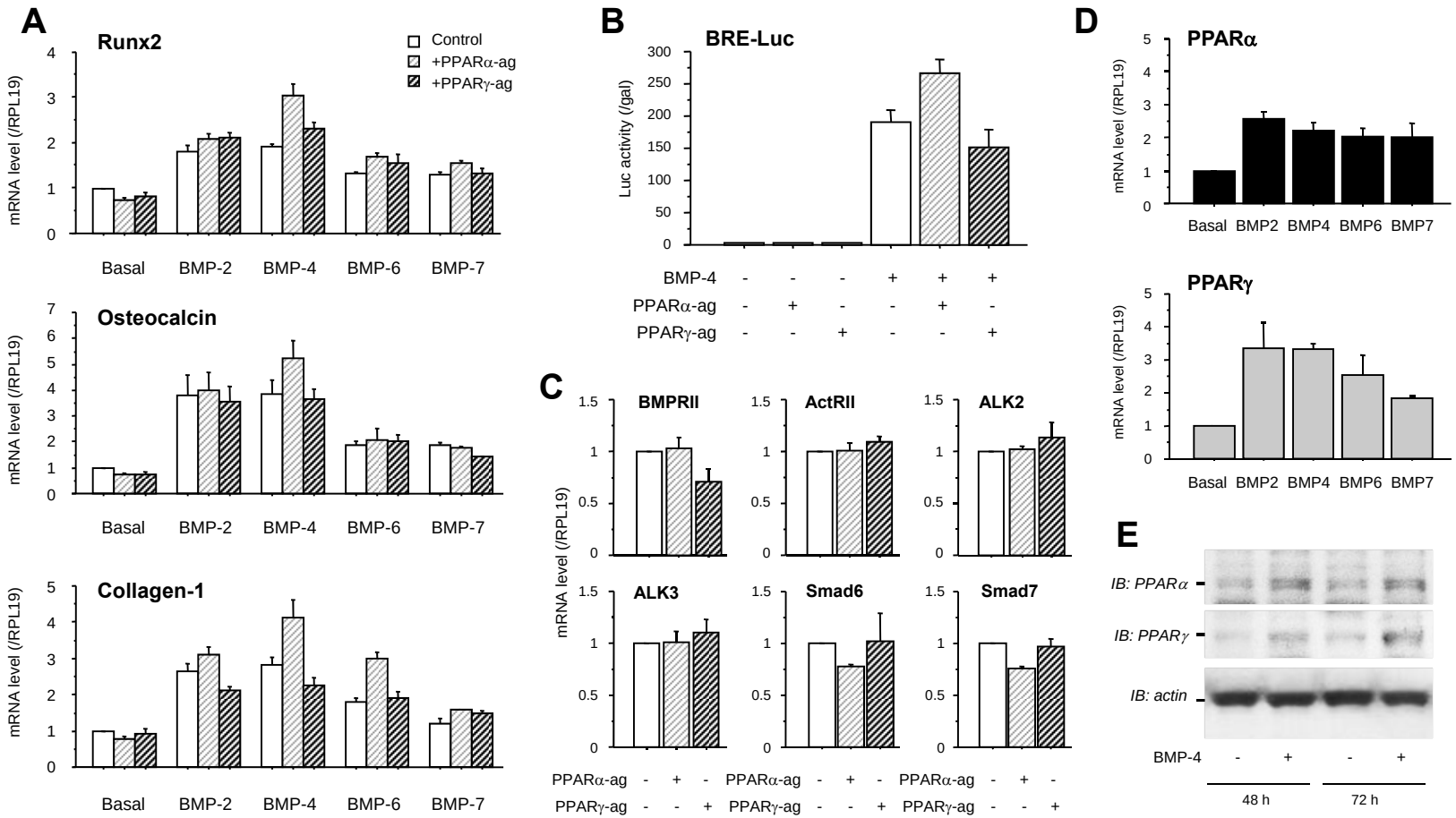
A
Runx2
Control
+PPARα-ag
+PPARγ-ag
mRNA level (/RPL19)
Basal
BMP-2
BMP-4
BMP-6
BMP-7
Osteocalcin
Collagen-1
B
BRE-Luc
Luc activity (/gal)
BMP-4
PPARα-ag
PPARγ-ag
C
BMPRII
ActRII
ALK2
ALK3
Smad6
Smad7
D
PPARα
PPARγ
E
IB: PPARα
IB: PPARγ
IB: actin
48 h
72 h

Fig. 2

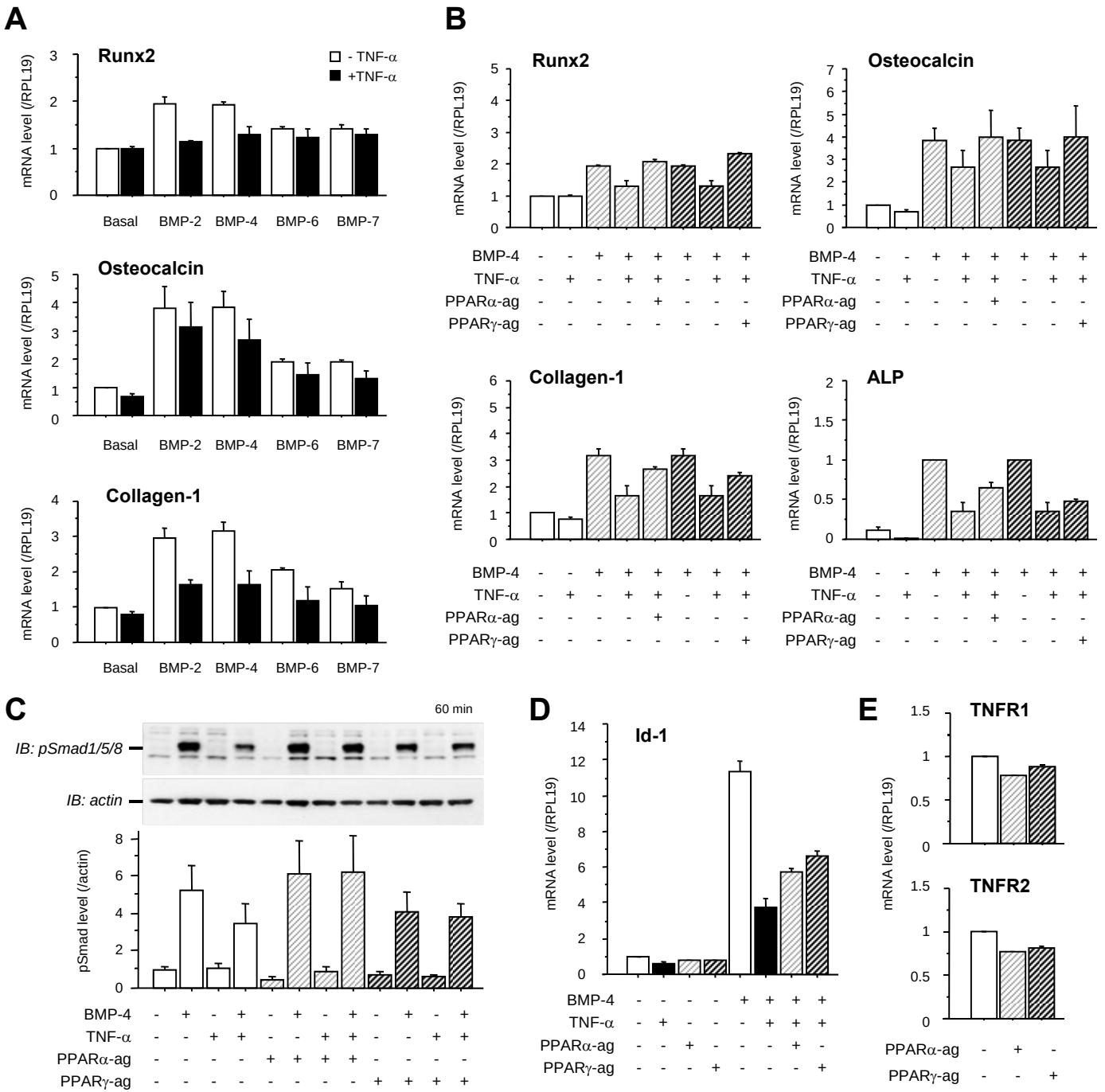
A
Runx2
- TNF-α
+TNF-α
mRNA level (/RPL19)
Basal
BMP-2
BMP-4
BMP-6
BMP-7
Osteocalcin
Collagen-1
B
Runx2
Osteocalcin
Collagen-1
ALP
BMP-4
TNF-α
PPARα-ag
PPARγ-ag
C
60 min
IB: pSmad1/5/8
IB: actin
pSmad level (/actin)
D
Id-1
E
TNFR1
TNFR2

Fig. 3

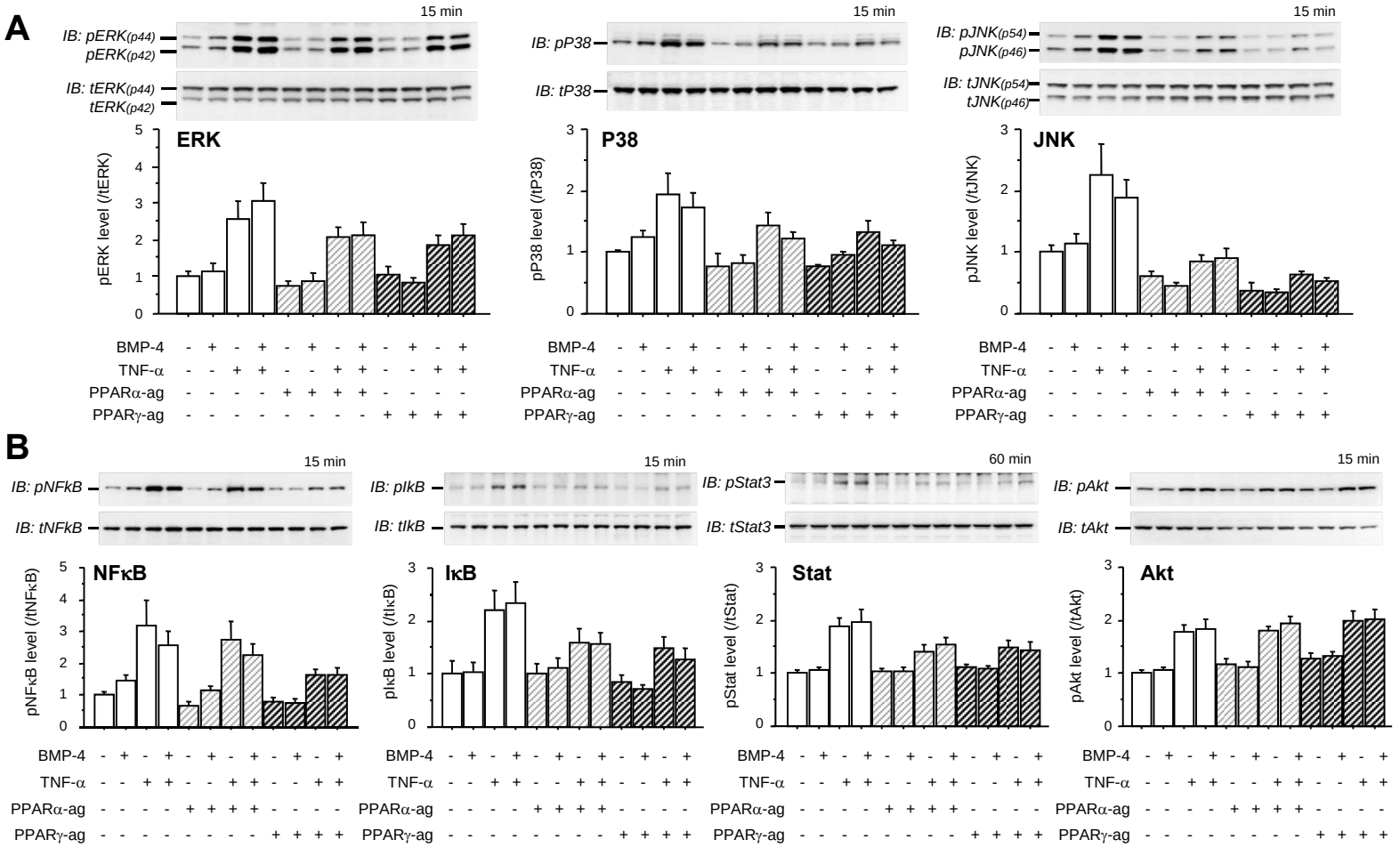
A
15 min
IB: pERK(p44)
pERK(p42)
IB: tERK(p44)
tERK(p42)
ERK
pERK level (/tERK)
IB: pP38
IB: tP38
P38
pP38 level (/tP38)
IB: pJNK(p54)
pJNK(p46)
IB: tJNK(p54)
tJNK(p46)
JNK
pJNK level (/tJNK)
BMP-4
TNF-α
PPARα-ag
PPARγ-ag
B
15 min
60 min
IB: pNFkB
IB: tNFkB
NFκB
pNFκB level (/tNFκB)
IB: pIkB
IB: tIkB
IκB
pIκB level (/tIκB)
IB: pStat3
IB: tStat3
Stat
pStat level (/tStat)
IB: pAkt
IB: tAkt
Akt
pAkt level (/tAkt)

Fig. 4

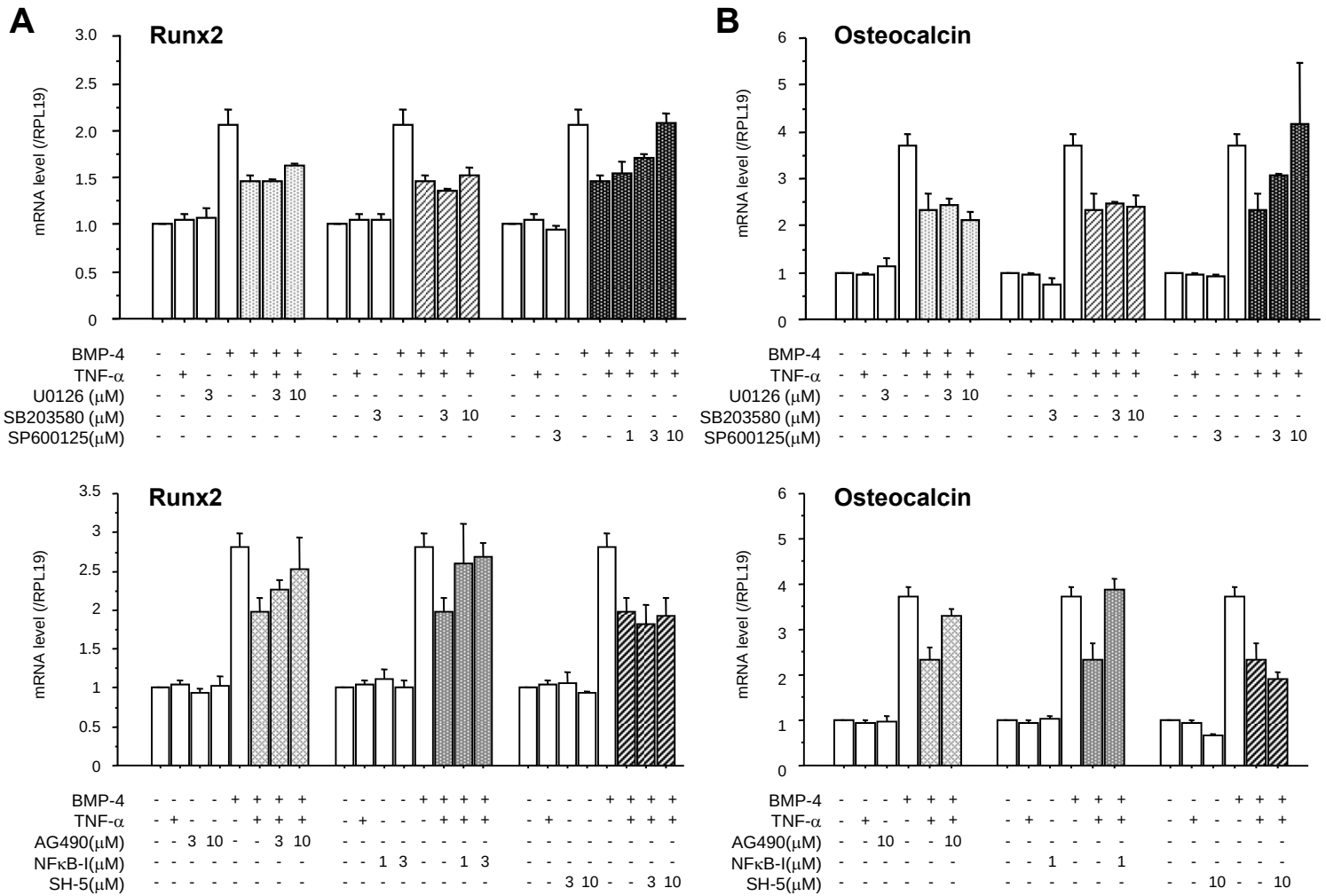
A
Runx2
mRNA level (/RPL19)
BMP-4
TNF-α
U0126 (μM)
SB203580 (μM)
SP600125(μM)
B
Osteocalcin
mRNA level (/RPL19)
BMP-4
TNF-α
U0126 (μM)
SB203580 (μM)
SP600125(μM)
Runx2
mRNA level (/RPL19)
BMP-4
TNF-α
AG490(μM)
NFκB-I(μM)
SH-5(μM)
Osteocalcin
mRNA level (/RPL19)
BMP-4
TNF-α
AG490(μM)
NFκB-I(μM)
SH-5(μM)

Fig. 5

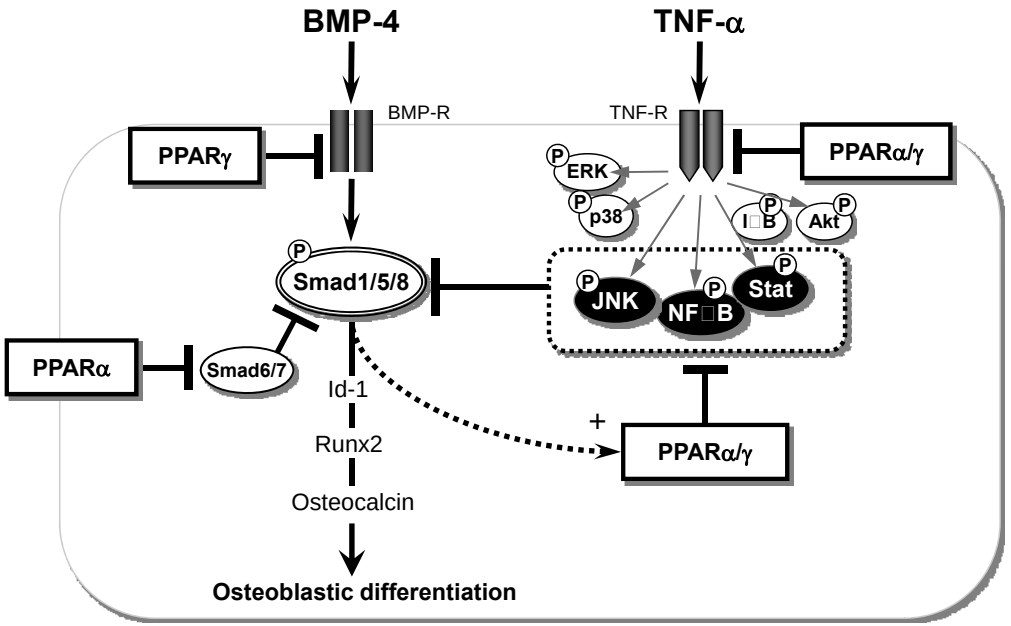
BMP-4
TNF-α
BMP-R
TNF-R
PPARγ
PPARα/γ
ERK
p38
IκB
Akt
Smad1/5/8
JNK
NFκB
Stat
PPARα
Smad6/7
Id-1
+
Runx2
PPARα/γ
Osteocalcin
Osteoblastic differentiation